Molecular Biology of the Cell
Vol. 18, 1530–1542, April 2007

# Impaired Fertility and Spermiogenetic Disorders with Loss of Cell Adhesion in Male Mice Expressing an Interfering Rap1 Mutant

**Evanthia Aivatiadou,* Elisabetta Mattei,† Michela Ceriani,‡ Leila Tilia,† and Giovanna Berruti***

*Laboratory of Cellular and Molecular Biology of Reproduction, Department of Biology, University of Milan, 20133 Milan, Italy; †Institute of Neurobiology and Molecular Medicine, Consiglio Nazionale delle Ricerche, 00143 Rome, Italy; and ‡Department of Biotechnology and Biosciences, University of Milano-Bicocca, 20126 Milan, Italy

Submitted October 10, 2006; Revised January 29, 2007; Accepted February 2, 2007
Monitoring Editor: Asma Nusrat

**The guanosine trisphosphatase Rap1 serves as a critical player in signal transduction, somatic cell proliferation and differentiation, and cell–cell adhesion by acting through distinct mechanisms. During mouse spermiogenesis, Rap1 is activated and forms a signaling complex with its effector, the serine-threonine kinase B-Raf. To investigate the functional role of Rap1 in male germ cell differentiation, we generated transgenic mice expressing an inactive Rap1 mutant selectively in differentiating spermatids. This expression resulted in a derailment of spermiogenesis due to an anomalous release of immature round spermatids from the seminiferous epithelium within the tubule lumen and in low sperm counts. These spermiogenetic disorders correlated with impaired fertility, with the transgenic males being severely subfertile. Because mutant testis exhibited perturbations in ectoplasmic specializations (ESs), a Sertoli–germ cell-specific adherens junction, we searched for expression of vascular endothelial cadherin (VE-cadherin), an adhesion molecule regulated by Rap1, in spermatogenic cells of wild-type and mutant mice. We found that germ cells express VE-cadherin with a timing strictly related to apical ES formation and function; immature, VE-cadherin–positive spermatids were, however, prematurely released in the transgenic testis. In conclusion, interfering with Rap1 function during spermiogenesis leads to reduced fertility by impairment of germ–Sertoli cell contacts; our transgenic mouse provides an in vivo model to study the regulation of ES dynamics.**

## INTRODUCTION

Spermatogenesis is the developmental program that guides spermatogonial stem cells to differentiate into functional spermatozoa. The dissection of the molecular mechanisms that regulate the mitotic (spermatogonia), meiotic (spermatocytes), differentiative (spermatids), and spermiation (spermatozoa) phases is useful for a comprehensive knowledge about the molecular requirements for correct spermatogenesis. This implies also a better understanding of the disorders related to male sterility and infertility, a pathology that is continuously growing in the Western world and that affects 15% of human couples (Cooke and Saunders, 2002). Spermatogenic failures are often based on lack of spermatogonial divisions (Blume-Jensen *et al*., 2000), on meiotic blocks (Nakai *et al*., 2000), and, more frequently, on cytomorphogenic derailment, which leads to the release of immature forms or aberrant spermatozoa (Kang-Decker *et al*., 2001; Giorgini *et al*., 2002). A significant improvement in our understanding of spermatogenesis can be provided by the emerging male germ cell culture technology (Kubota *et al*., 2004). Sperm development occurs, however, physiologically within the testis where the somatic Sertoli cells play a crucial role by providing essential structural and nutritive supports. The process, therefore, could not be entirely reconstructed or understood in vitro; moreover, we, still need to transplant cultured germ cells to the seminiferous tubules of recipient animals to complete donor-derived spermatogenesis (Kubota *et al*., 2004). Animal models are always necessary for dissecting in vivo the effective role of a molecular player thought to be crucial for the process.

Rap1 is a small guanosine trisphosphatase (GTPase) of the Ras family (Kitayama *et al*., 1989) that is involved in regulation of morphogenesis (Asha *et al*., 1999; Ji and Andrisani, 2005) and somatic cell differentiation (Vossler *et al*., 1997; Zhu *et al*., 2002). Rap1 is recently attracting attention because of its role in regulating cell–cell adhesion (Bos, 2005). The GTPase cycles between an inactive GDP-bound and an active GTP-bound conformation, becoming active in response to various extracellular stimuli by way of Rap1-specific guanine nucleotide exchange factors (GEFs) (Zwartkruis and Bos, 1999). Dominant-negative mutants have been useful in deciphering some Rap1-dependent pathways, because by trapping GEFs, they are no longer able to activate downstream effectors (Feig, 1999). For example, the Rap1[S17N] mutant has been instrumental in revealing the cAMP–Rap1–B–Raf/extracellular signal-regulated kinase pathway (Vossler *et al*., l997; Schmitt and Stork, 2000).

This article was published online ahead of print in *MBC in Press* (http://www.molbiolcell.org/cgi/doi/10.1091/mbc.E06–10–0902) on February 21, 2007.

Address correspondence to: Giovanna Berruti (giovanna.berruti@unimi.it).

Abbreviations used: ES, ectoplasmic specialization.

We showed previously that Rap1 is expressed in spermatogenic cells; in differentiating spermatids, Rap1 was found to be complexed in vivo with its effector 95-kDa B-Raf and the molecular adaptor 14-3-3 $\theta$ protein (Berruti, 2000). We thus suggested an involvement of Rap1 in the process of sperm differentiation. To explore such a possibility, we have generated transgenic mice with a dominant-negative mutant of Rap1 under the control of the haploid germ cell-specific *Protamine-1* promoter so as to achieve both tissue and temporal restriction in the expression of the transgene. Using this approach, we found that interfering with Rap1 specifically in haploid cells results in an anomalous release of immature spermatids within the lumen of seminiferous tubuli and in low sperm counts; the loss of nondifferentiated cells correlated with impaired spermatid–Sertoli cell adhesion. We thus searched for the presence in male germ cells of an adhesion molecule whose function at cell–cell contacts in somatic cells is known to be regulated by Rap1; we found that male germ cells express vascular endothelial cadherin (VE-cadherin) with a timing that is coincident with the formation and function of apical ectoplasmic specialization (ES), the highly dynamic testis and Sertoli–spermatid-specific adherens junction.

## MATERIALS AND METHODS

### *Generation of Transgenic Construct*

The plasmid bPGV-mPI-RapS17N, containing the human Rap1A S17N (dominant negative) tagged with hemagglutinin (HA), under the control of mouse *Protamine-1* (*Prm-1*) promoter, was constructed using standard cloning procedures (Sambrook *et al*., 1989). The plasmid pMT-2 containing the human Rap1A S17N tagged with HA at its amino terminus (van den Berghe *et al*., 1997) was digested with EcoR1 and HindIII (New England Biolabs, Ipswich, MA), and the 900-base pair fragment, containing the full-length cDNA coding for HA-Rap1A S17N, was separated on agarose gel electrophoresis and purified with JETSORB gel extraction kit (Genomed, Löhne, Germany). The plasmid bPGV-mPI (Yamazaki *et al*., 1998), containing the *Prm-1* enhancer region, the firefly luciferase reporting gene, and simian virus 40 (SV40) polyA region, was digested with EcoR1 and HindIII and used for subcloning the 900-base pair HA–Rap1 S17N fragment. The bPGV-mPI-Rap1S17N plasmid so obtained contains the human HA-Rap1 S17N under the control of a portion (from −318 to +30) of the *Prm-1* promoter, a fragment of luciferase coding sequence, and the SV40 polyadenylation signal. The fusion between *Prm-1* promoter and HA-Rap1S17N was controlled by sequencing. This plasmid was then digested with BamH1, Fsp1, and BstX1 and electrophoresed through genetic technology grade agarose (Seakem GTG; BMA, Rockland, ME). The band corresponding to the transgenic insert (3356 base pairs), containing the *Prm*1-HA-Rap1S17N fusion, a fragment of luciferase cDNA, and polyA site of SV40, was cut out, and the DNA was recovered from agarose by QIAquick gel extraction kit (QIAGEN, Milan, Italy) according to the manufacturer's instructions. The transgenic fragment was dissolved in injection buffer (10 mM Tris, pH 7.5, 0.1 mM EDTA, and 30 mM NaCl).

### *Mice*

BDF1 (C57Black6 × DBA) mice were purchased from Charles River Italia (Calco, Italy). They were housed under conventional, controlled standard conditions and killed by carbon dioxide asphyxiation. Transgenic mice were generated by microinjecting the HA–Rap1 S17N fragment at a concentration of 3.5 ng/ml into the pronuclei of fertilized eggs derived from BDF1 × BDF1 matings. Pseudopregnant foster females from the same strain were used for oviduct implantation of embryos that survived microinjection. Transgenic animals were identified by polymerase chain reaction (PCR).

The transgenic lines were maintained by crossing founder females (F0) and F1 hemizygous females with wild-type BDF1 males. F1 and F2 transgenic hemizygous males and their wild-type littermates were used for experiments. Transgenic colonies were housed under a 12-h light/dark schedule, and they were fed a standard rodent chow. All protocols for animal care, handling, and euthanasia were in accordance with policies on the care and use of animals promulgated by the ethical committee of the University of Milano following the guidelines of the Italian Minister of Health, DL 27 January 1992, No. 116.

### *PCR and Reverse Transcription-Polymerase Chain Reaction (RT-PCR)*

Identification of transgenic founders was carried out by nested PCR analysis. A small piece of mouse tail was excised, and genomic DNA was extracted by proteinase K-SDS as described previously (Nagy *et al*., 2003). Fifty nanograms of DNA was used for PCR analysis. A first round of amplification was performed using primer P1 (5′-CCTCTTTGACTTCATAATTCCTAGGGGC-3′) and primer R2 (5′-TTCTGGCCCTGCTCTTTGCCAACTAC-3′) and *Taq* polymerase (Invitrogen). These two oligonucleotides amplify a 700-base pair fragment comprising a region starting in the mouse *Pmr*-1 promoter (accession no. X07625) and ending in the middle of human Rap1 sequence (accession no. NM_001010935). One microliter of the first amplification mixture was then used for a second round of PCR by using P1 and R1 (5′-CCTGAAC-CAAGGACCACTAGCTTGTG-3′) oligonucleotides. A 350-base pair fragment starting in the *Pmr-1* promoter and ending in the beginning of Rap1 gene is the result of the second amplification. We used a nested PCR procedure, because artifacts and unspecific amplification products were observed frequently by using only one round of PCR. As a positive control, we used a small amount (0.1 ng) of bPGV-mPI-Rap1S17N plasmid. Positive founders also were tested and confirmed by Southern blot analysis by using a firefly luciferase probe obtained by digesting pGL3-Basic vector (Promega, Madison, WI) with XhoI and XbaI. This process was followed by gel electrophoresis to recover the luciferase sequence (1710 base pairs), which was eluted from the agarose by QIAquick gel extraction kit (QIAGEN).

RNA was extracted from freshly isolated tissues, purified populations of spermatogenic cells (see below), or both by using TRIzol reagent (Invitrogen, Carlsbad, CA) according to the manufacturer's instructions. RT-PCR assays were performed using 1 $\mu$g of total RNA and Invitrogen SuperScript III first-strand synthesis system for RT-PCR. In particular, to convert poly(A)$^+$-mRNA into first-strand cDNA, 1 $\mu$g of total RNA was combined with 5 $\mu$M oligo(dT)$_{20}$, 1 mM dNTP mix, and diethyl pyrocarbonate-treated water in a final volume of 10 $\mu$l; the mix was incubated at 65°C for 5 min and placed on ice for 1 min. Each sample was then added to 10 $\mu$l of cDNA synthesis mix (2 $\mu$l of 10× reverse transcriptase [RT] buffer, 4 $\mu$l of 25 mM $MgCl_2$, 2 $\mu$l of 0.1 M dithiothreitol, 1 $\mu$l of 40 U/$\mu$l RNaseOUT, and 1 $\mu$l of 200 U/$\mu$l SuperScript III RT) and incubated at 50°C for 50 min. The reaction was finally incubated at 85°C for 5 min. Thereafter, each PCR reaction was performed with 2 $\mu$l of RT product by using P2 (5′-GCTTACCCATACGATGTTCCAGATTACGCG-3′) and R2 (see above) oligonucleotides; these primers amplify a 400-base pair cDNA fragment that comprises a region starting in the HA coding sequence (van den Berghe *et al*., 1997) and ending in the middle of Rap1A sequence. Primers selected for mouse VE-cadherin transcript were MmCadh1 (5′-GGATGCAGAGGCTCACAGAGCTGG-3′) and MmCadh2 (5′-CTTAGCAT-TCTGGCGGTTCACGTTGGAC-3′) that amplify a 211-base pair fragment specific for mouse VE-cadherin mRNA (accession no. NM_009868.3).

### *Cell Culture and Transfection*

COS 7 cells were grown at 37°C in Dulbecco modified Eagle's medium (Invitrogen) supplemented with 10% heat-inactivated fetal bovine serum (Euro Clone, Pero, Italy). COS 7 were plated at a density of $5 \times 10^6$ cells/60-mm dish, 1 d before transfection. Cells were transiently transfected with 6 $\mu$g of pCDNA3-Rap1-HA plasmid (De Rooij *et al*., 1998) by using Lipofectamine (Invitrogen).

### *Protein Extracts and Western Blot Analysis*

Testes from 16-, 28-, 35-d-old, and adult transgenic and wild-type mice were used to obtain spermatogenic cells isolated by sequential enzymatic treatments essentially as described previously (Berruti, 2000, 2003). Total testis homogenates were obtained as described previously (Berruti, 2000). For immunodetection of endogenous and transgenic Rap1, cells were lysed in 50 mM Tris, 100 mM NaCl, 2 mM EDTA, pH 7.8, containing 0.1% Triton X-100, and 100 $\mu$g/ml leupeptin and aprotinin plus a Complete protease inhibitor cocktail (Sigma-Aldrich, St. Louis, MO) (Berruti, 2000). Equal amounts of protein were loaded on 12% polyacrylamide-SDS gels and blotted. Proteins were detected with one of the following antibodies: rabbit anti-Rap1 (sc-65; Santa Cruz Biotechnology, Santa Cruz, CA), mouse monoclonal anti-Rap1 (catalog no. 610196; BD Biosciences, San Jose, CA), rabbit anti-HA (sc-805; Santa Cruz Biotechnology), and mouse monoclonal anti-HA (catalog no. 1583816; Roche Diagnostics, Mannheim, Germany). Secondary anti-rabbit or anti-mouse immunoglobulin Gs (IgGs) conjugated to horseradish peroxidase were from GE Healthcare (Little Chalfont, Buckinghamshire, United Kingdom). The enhanced chemiluminescence detection system (Pierce Chemical, Rockford, IL) was used to visualize immunoreactive bands. For VE-cadherin expression assays, germ cells, isolated by sequential enzymatic treatments of decapsulated adult testes, were recovered by filtration through nylon meshes with 100- and 40-$\mu$m pores (BD Biosciences) to eliminate cell clumps and somatic cell contamination (Aravindan *et al*., 1996). The purity of germ cell preparations was assessed carefully by a combination of two procedures, i.e., direct microscopic examination for exclusion of Sertoli cells in the preparation and immunoblotting with mouse monoclonal anti-c-kitL (sc-13126; Santa Cruz Biotechnology) for c-kitL (a Sertoli cell marker) immunonegativity. Cells were lysed in 50 mM Tris, 100 mM NaCl, and 2 mM EDTA, pH 7.8, containing 1% Triton X-100 and protease inhibitors, and proteins were loaded on an 8% polyacrylamide-SDS gel to be immunoprobed with goat anti-VE-cadherin (sc-6458l; Santa Cruz Biotechnology), followed by anti-goat IgGs conjugated to horseradish peroxidase (GE Healthcare).

### *Isolation of Seminiferous Tubules, Protein Partition, and Immunoprecipitation*

Seminiferous tubules were isolated from 30-d-old testes of both transgenic and wild-type mice following standard procedures (Lee *et al*., 2003). Briefly, testes were decapsulated, and tubules were isolated by enzymatic digestion by using collagenase (0.05%, wt/vol) treatment (6–7 min at 34°C, under gentle shaking). The enzyme solution was decanted, and interstitial cells were removed by washings in RPMI 1640 medium by sedimentation under unit gravity. For partitioning proteins into soluble and insoluble fractions, an aliquot of seminiferous tubules was withdrawn, pelleted by centrifugation at 200 × *g*, and resuspended in homogenizing buffer (10 mM Tris and 150 mM NaCl, pH 7.5, containing 0.05% Triton X-100 plus a Complete protease inhibitor cocktail) to be immediately transferred to a glass microhomogenizer. The tubules were thoroughly homogenized on ice, and the resulting lysate was clarified by centrifugation for 10 min at 12,000 × *g*. The resulting supernatant is the soluble homogenate fraction. The respective pellet was resuspended in detergent buffer (10 mM Tris and 150 mM NaCl, pH 7.5, added with 0.5% Triton X-100 and 0.1% SDS [wt/vol] as final concentrations and protease inhibitors), sonicated, and allowed to continue on a rotating platform for 20 min at 4°C. After centrifugation, the resulting supernatant is the detergent homogenate fraction. In parallel, another aliquot of the seminiferous tubules was directly incubated in the detergent buffer, homogenized, and then processed as described above for the detergent homogenate fraction; its clarified lysate is the total homogenate fraction. Protein concentration was determined using a protein assay (Bio-Rad DC Protein Assay; Bio-Rad, Hercules, CA).

Pervanadate (PV) is a potent inhibitor of phospho-tyrosine phosphatases, and according to Lampugnani *et al*. (1997), to maintain phosphorylated tyrosine residues in VE-cadherin, cells have to be treated with a combination of vanadate and hydrogen peroxide before protein extraction. So, after collagenase digestion, seminiferous tubules from 30-d-old testes of both transgenic and wild-type mice were washed four times with RPMI 1640 medium containing 100 μM vanadate and 200 μM hydrogen peroxide. Extraction buffer, i.e., the detergent buffer reported above, and all the subsequent buffers used for these samples also contained 300 μM vanadate and 600 μM hydrogen peroxide. Control samples were subjected to the same treatments, with the exception of the addition of vanadate and hydrogen peroxide. For each immunoprecipitation (IP) assay, 600 μg of protein of seminiferous tubuli total lysate was first precleared on protein A-Sepharose (Sigma-Aldrich) for 30 min at 4°C. Supernatants were collected and incubated with either the mouse monoclonal anti-phospho-tyrosine 4G10 antibody (catalog no. 05-321; Upstate Biotechnology, Lake Placid, NY) or mouse preimmune serum (Sigma-Aldrich) for 2 h at 4°C on a rotating platform, followed by a further incubation in the presence of protein A-Sepharose under the same conditions to precipitate the immunocomplexes. After two washings with the respective IP buffers and a further two washings with ice-cold 10 mM Tris-HCl, 150 mM NaCl containing vanadate and hydrogen peroxide for samples treated in vivo with PV, the immunoprecipitated complexes were resuspended in 2X SDS-polyacrylamide gel electrophoresis (PAGE) sample buffer and boiled for 8 min to elute bound proteins. Protein separation by SDS-PAGE was followed by electrotransfer to nitrocellulose sheets.

### *Histology and Immunohistochemistry*

A single testis and epididymis from each animal was fixed overnight at 4°C in Bouin's fixative, embedded in paraffin wax, and sectioned at a thickness of 5 μm. For routine histology, sections were stained with hematoxylin and eosin according to standard protocols. Tubules from adult testis were classified into the specific stages according to the classification of Oakberg (1956). For immunohistochemistry, endogenous peroxidase activity was quenched in 0.3% $H_2O_2$ for 15 min. Sections were treated with primary antibody, followed by anti-rabbit (Chemicon International, Temecula, CA) or anti-goat (GE Healthcare) horseradish peroxidase-conjugated secondary antibody and Vector NovaRED substrate kit (Vector Laboratories, Burlingame, CA). In controls, primary antibody was replaced with either neutralized primary antibody (anti-HA-[Santa Cruz Biotechnology] neutralized with its blocking peptide [sc-805 P; Santa Cruz Biotechnology]) or goat normal serum (Sigma-Aldrich). Occasionally, sections were counterstained with hematoxylin (Vector Laboratories).

### *Immunofluorescence*

After blocking of nonspecific binding sites in 3% bovine serum albumin in phosphate-buffered saline for 1 h at room temperature, deparaffinized 5-μm sections of testis were incubated with goat anti-VE-cadherin antibody, followed by anti-goat Alexa 488-conjugated IgG secondary antibody (Invitrogen) for immunofluorescence analysis. In control samples, primary antibody was replaced with goat normal serum. Nuclei counterstaining was carried out with 3 μg/ml 4′,6-diamidino-2-phenylindole (DAPI) (Sigma-Aldrich).

Spermatogenic cell suspensions, prepared according to the protocol for double-label immunofluorescence described in detail previously (Berruti and Martegani, 2001), were smeared on slides, methanol fixed, processed for blocking of nonspecific sites, and then immunostained with the anti-VE-cadherin antibody, followed by the Alexa 488-conjugated IgG as the secondary antibody. In control samples, primary antibody was replaced with goat normal serum. Nuclei counterstaining was carried out with 2 μg/ml DAPI.

Cells and sections were examined on a Nikon Eclipse E 600 microscope equipped with standard filter sets for green (Alexa 488) and blue (DAPI) fluorescence. Images were acquired with a Leica DG350F charge-coupled device camera (Leica Microsystems, Deerfield, IL) by using Imaging software (Microsoft Corporation, Redmond, WA) and elaborated with Adobe Photoshop (Mountain View, CA).

### *Sperm Counts and Analysis*

Sperm counts were made on epididymal sperm released from a single epididymis of each animal. The second epididymis was processed for histological analysis. The epididymis was minced in 1 ml of sperm motility buffer (Holdcraft and Braun, 2004), and sperm were allowed to swim out for 2 h at room temperature. Numbers of epididymal sperm were determined by hemocytometer counts either undiluted or diluted 10-fold. All counts were made in duplicate and averaged.

Sperm morphology was routinely analyzed using phase-contrast microscopy with live cells and hematoxylin and eosin staining with fixed cells. For scanning electron microscopy, isolated epididymal spermatozoa were processed and examined as described previously (Mashiach *et al*., 1992).

### *Estimation of Round and Elongating/Elongated Spermatid Populations in Typical Cross Sections*

Observations for counts were made on Bouin-fixed, paraffin-embedded, hematoxylin and eosin-stained 5-μm testis sections, examined at 40× magnification on a Leica DME microscope. Cross sections of seminiferous tubules at stages I–VI, VII–VIII, and IX–XII (Oakberg, 1956) were randomly selected, and the images were acquired using a Leica DC 150 camera coupled to a personal computer. At least 20 cross sections for each stage group were examined from each testis (2 testes from 2 3-mo-old transgenic mice and 2 testes from their wild-type littermates).

### *Statistical Analysis*

Paired comparisons of different fertility parameters and of the counts of round and elongating/elongated spermatids in randomly selected testis sections between wild-type and transgenic male mice were performed for statistical significance by chi-square test and Student's *t* test.

## RESULTS

### *Generation of Transgenic Mice Expressing a Developmentally Controlled Dominant-Negative Rap1 in the Testis*

To investigate the possible involvement of Rap1 GTPase in mammalian spermiogenesis in vivo, we generated transgenic mouse lines in which a dominant-inhibitory mutant of Rap1, Rap1S17N, was expressed in differentiating spermatids.

Expression of the transgene was driven by the spermatid-specific *Protamine-1* promoter that becomes active after day 20 postpartum (P) (Peschon *et al*., 1987; Zambrowicz *et al*., 1993). As revealed by the sequencing of the transgenic construct, the *Protamine-1* promoter region used resulted to be 348 base pairs and included the sequence from −318 to +30 base pairs of the numeration according to Zambrowicz *et al*. (1993). This sequence contains both the 113-base pair region that directs spermatid-specific transcription and the box C required for high-level transcription (Zambrowicz *et al*., 1993). The full-length Rap1S17N cDNA brings an HA tag of 27 base pairs at its N terminus.

The interfering Rap1 (iRap1) founder lines were identified by nested PCR amplification of regions specific to the transgene junction. Four independent mouse lines, TGRap1, TGRap3, TGRap9, and TGRap11, were established (Figure 1A). When the founder animals were females (the last three transgenic lines), no problem was encountered in obtaining offspring; in contrast, this was not the case with the TGRap1 male founder. Notwithstanding this male was caged with multiple females for >3 mo, only three matings were successful, but they produced no transgenic offspring. This line was thus neglected.

Transgenic mRNA in germ cells of hemizygous male offspring from female founders bred with wild-type males was

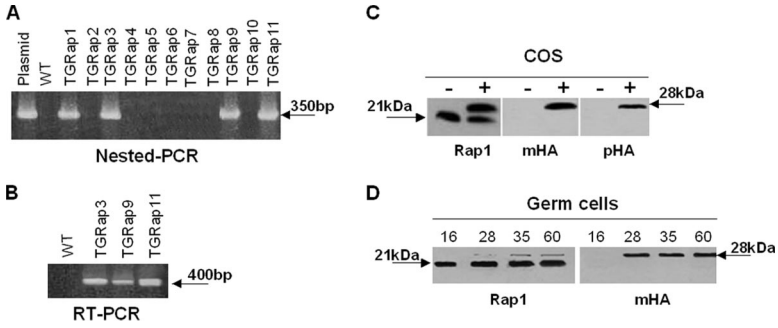


**Figure 1.** Characterization of transgenic iRap1 mice. (A) PCR genotyping with selected primers to detect the 350-base pair transgenic fragment in the founder lines (TGRap1-TGRap11); as a positive control, the bPGV-mPI-Rap1S17N-HA plasmid (first lane); as a negative control, DNA extracted from a wild-type mouse (second lane). (B) The 400-base pair transgenic transcript was detected by RT-PCR analysis in germ cells of F1TGRap3, F1TGRap9, and F1TGRap11 male mice. A wild-type (WT) male gave no transcript. (C) Western blots of COS cells, transfected (+) or not (−) with pCDNA3-Rap1-HA plasmid, probed with anti-Rap1 antibodies (left), monoclonal (mHA), anti-HA antibodies (middle), and polyclonal (pHA) anti-HA antibodies (right). (D) Western blots of germ cells from 16-, 28-, 35-, and 60-d-old transgenic testes probed with anti-Rap1 antibodies (left) and anti-HA antibodies (right). The mutant protein is detectable starting from 28-d-old testis.

detected by amplifying Rap1S17N–HA-specific sequences by RT-PCR. Genotyped F1 males from TGRap3, TGRap9, and TG Rap11 families showed the expected transcript of 400 base pairs but not at comparable levels (Figure 1B); a wild-type animal gave no transcript (Figure 1B, lane WT). RT-PCR assays carried out with RNA extracted from brain, liver, and kidney were used to determine whether the transgene was expressed in somatic tissues; none yielded the transgenic transcript (data not shown).

We then selected the line with the apparent highest level of iRap1mRNA (TGRap11) to assess the expression of the mutant protein. Because the Rap1 mutant is expected to be translated only in a limited fraction of the total cells from sexually mature transgenic testis, we selected the immunoblotting conditions carefully. By exploiting the small HA epitope tag of Rap1S17N protein, we probed a panel of commercial anti-HA antibodies on protein extracts first from COS cells, transfected or not with the pCDNA3-Rap1-HA plasmid, to check the antibody(ies) that gave the best signal-to-noise ratio, and then we probed germ cells isolated from transgenic testes. Parallel immunoblots were probed with anti-Rap1 antibodies. Figure 1, C and D, shows the relative immunoblots. As shown in Figure 1D, the HA-tagged-Rap1 signal was immunorevealed in the 28-d-old, 35-d-old, and adult transgenic testis, i.e., respectively, from mice that are carrying out their first cycle of haploid differentiation, had just completed the first wave of the spermatogenic cycle, and are adults. On the contrary, the 16-d-old transgenic testis (meiotic phase) gave no HA-tagged Rap1 signal.

### *Reduced Fertility in iRap1 Male Mice*

As mentioned above, the male founder TGRap1 was seriously subfertile, notwithstanding its mating behavior was apparently normal and the mating produced generally copulatory plugs in the wild-type female partners. Its offspring did not result in any transgenic litters. TGRap1 was killed at 6 mo; its testes showed a heavily altered histology (Figure 2A), whereas epididymal spermatozoa displayed sluggish movement and an unusual number of head abnormalities as a hammer-shaped or ovoid head (Figure 2, B–D). Founder and F1 hemizygous transgenic females (TGRap3, TGRap9, and TGRap11) displayed normal fertility. The F1 transgenic males from these lines, when mated with wild-type females, exhibited normal sexual behavior and originated offspring. We noticed no significant difference in mean sizes of testes and epididymes among TGRap3, TGRap9, and TGRap11 male mice and wild-type males, when matched for age. On the contrary, epididymal sperm counts from the transgenic animals were significantly lower compared with wild-type littermates (Table 1). Although the TGRap males were apparently fertile, the percentages of their successful 7-d timed mating experiments were remarkably lower compared with the wild type (Table 1); moreover, the successful mating with transgenic males originated less pups compared to that with wild-type littermates (Table 1). On the whole, epididymal sperm counts and fertility parameters correlated with the levels of transgene expression (Table 1).

### *Impaired Spermiogenesis in Mice Expressing Rap1S17N-HA*

To elucidate the nature of the defect in fertility parameters of male mice expressing the Rap1 mutant protein, we performed a detailed histological analysis of the testis. In all of the experiments described below, F1 and F2 mice from iRap1 transgenic lines were examined, and they displayed similar phenotypes. The data reported in this study, how-

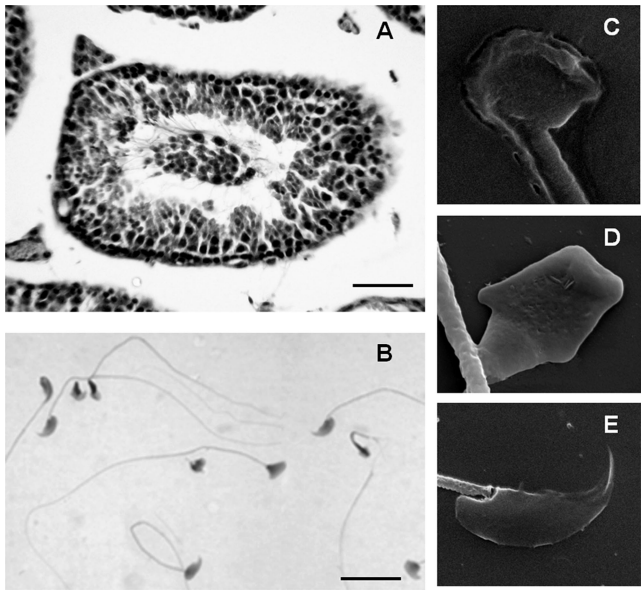


**Figure 2.** Analysis of testis histology and epididymal spermatozoa of the TGRap1 male founder. (A) Hematoxylin and eosin-stained section showing a heavily altered histology of the seminiferous epithelium and numerous immature cells released into the tubule lumen. Bar, 16 $\mu$m. (B) Cauda epididymal spermatozoa display severe head abnormalities, as a hammer-shaped or ovoid head. Bar, 10 $\mu$m. (C–E) Scanning electron micrographs of spermatozoa from TGRap1 founder (C and D), showing an ovoid and hammer-shaped head, respectively, and a wild-type head (E).

**Table 1.** Epididymal sperm counts and fertility parameters of male mice aged 3–4 mo

| Genotype | No. of successful matings[a] | Litter size[b] | Sperm count ($\times 10^6$/epi)[c] |
|---|---|---|---|
| Wild type | 12/12 | 10.70 ± 2.46 | 48.00 ± 1.41 (n = 4) |
| F1TGRap9 | 7/13[d] | 5.86 ± 1.07** | 16.70 ± 0.57 (n = 3)** |
| F1TGRap3 | 3/16[d] | 6.33 ± 0.57* | 8.40 ± 1.14 (n = 5)** |
| F1TGRap11 | 6/21[d] | 5.33 ± 0.82** | 5.43 ± 0.54 (n = 7)** |

epi, epididymus.

* Values are significantly different (*t* test, $p < 0.01$).

** Values are significantly different (*t* test, $p < 0.001$).

[a] Number of wild-type females impregnated after 7-d cohabitation.

[b] Average number of newborn pups. Values are mean ± SD.

[c] Values are mean ± SD for the number of mice indicated (n).

[d] Values are significantly different (chi-square test, $p < 0.05$).

ever, concern predominantly F1 mice, mainly from the TGRap11 line.

Histological examination of testis from 3-mo-old F1 TGRap3, F1 TGRap9, and F1 TGRap11 mice revealed that although spermatogenesis progresses to the latest steps, few released sperm could be found in the luminal compartment of seminiferous tubules, whereas numerous immature spermatids and/or occasional multinucleated cells were present (Figure 3, A, D, G, B, E, and H). Consistent with this finding was the epididymis histology: the presence of enlarge cells and few spermatozoa was a constant characteristic of the epididymal lumen of F1 TG Rap3, F1 TG Rap9, and F1 TG Rap11 males (Figure 3, C, F, and I), whereas this characteristic was observed only occasionally in the wild-type littermates (Figure 3M).

Testes and epididymes from transgenic and nontransgenic littermates of the TG Rap11 line were extensively examined, and the diverse spermatogenic stages were analyzed. Figure 4 shows some of these stages. Stage II, for example, is characterized by the presence of dividing spermatogonia and spermatids at steps 2 and 14 of spermiogenesis (Oakberg, 1956). Wild-type testis showed the canonical pattern for the stage II (Figure 4A), whereas the transgenic testis exhibited a reduction in the number of spermatids at step 14 (Figure 4B). Control stage VII contains preleptotene spermatocytes and spermatids at steps 7 and 16 (Figure 4C); in transgenic stage VII, the spermatocytes were normally present, but spermatids both at step 7 and 16 were reduced (compare Figure 4D with C). At the transition from stage X to stage XI, wild type shows spermatids at steps 10 and 11 (Figure 4E); these spermatids, albeit present, were in lower numbers in the transgene (Figure 4F). Evaluation of the number of round spermatids (steps 1–8) and elongating/elongated spermatids (steps 9–16) in seminiferous tubules indicated significant reductions in transgenic versus wild-type mice (Table 2).

So, although all spermatogenic stages were observed, transgenic testes displayed abnormal tubules coincident, regarding seminiferous epithelium, with reductions in the expected classes of spermatids, and, regarding tubule lumen, with the presence of exfoliated immature spermatids and low spermatozoa. In addition, Sertoli–germ cell contacts

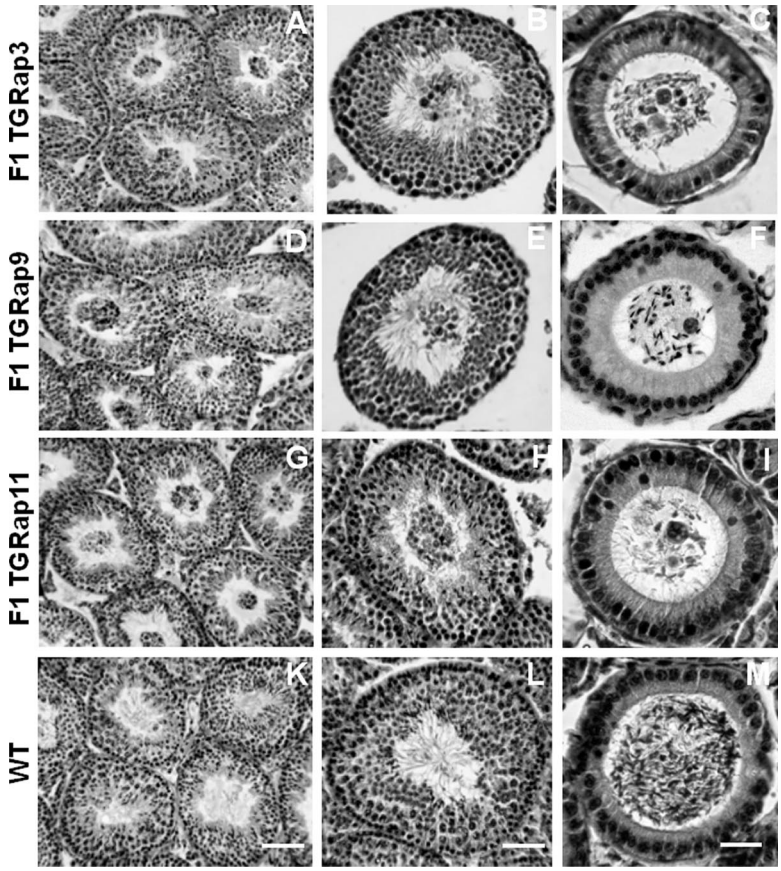


**Figure 3.** Histological examination of adult testis and epididymis. Sections of transgenic testes from F1 TGRap3 (A and B), F1 TGRap9 (D and E), and F1 TGRap11 (G and H) mice are characterized by common abnormalities as the unusual presence of immature spermatids and occasional enlarged round cells inside the tubule lumen and few released spermatozoa. Such abnormalities are found also in the epididymal lumen (C; F1 TGRap3; F, F1 TGRap9; and I, F1 TGRap11). For comparison, wild-type testis (K and L) and epididymis (M). Bar, 50 $\mu$m (A, D, G, and K), 27 $\mu$m (B, E, H, and L); and 18 $\mu$m (C, F, I, and M).

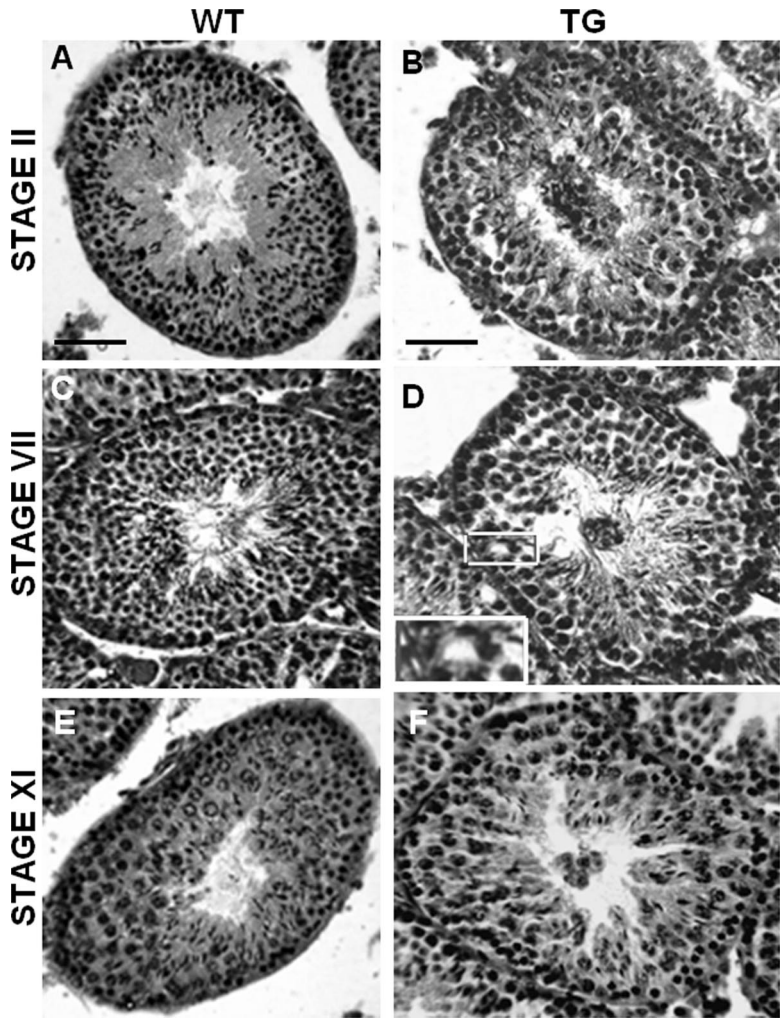


**Figure 4.** Histological comparison of stages of the seminiferous epithelial cycle between wild-type (WT column) and transgenic (TG column) testes. (A–F) Representative cross sections of stage II tubules (A and B), stage VII tubules (C and D), and stage XI tubules (E and F) are shown. Transgenic testes at all spermatogenic stages exhibit abnormal tubules, with a reduction in ordinary classes of expected spermatids, low numbers of spermatozoa, and the constant presence of differentiating spermatids immaturely released into the lumen. Moreover (D, boxed inset provides a higher magnification), Sertoli–germ cell contacts are often disturbed with a more or less serious loss of adhesion. Bar, 20 $\mu$m (A, C, and E) and 16 $\mu$m (B, D, and F).

were often found to be perturbed (Figure 4D, inset). For the epididymes, overall size and organization were apparently similar between transgenic and nontransgenic littermates. However, in line with data reported in Table 1 and Figure 3, mature sperm were constantly scanty in the mutant epididymal lumen where cellular debris and what seemed to be large, round spermatids were often observed (Figure 5, A and B, wild type; and C and D, iRap1).

**Table 2.** Spermatid numbers in cross sections from transgenic and wild-type seminiferous tubules

| Epithelium stages | Genotype | Round spermatids[a] | Elongating/ed spermatids[b] |
|---|---|---|---|
| I–VI | WT | 120.5 ± 6.50 | 125.5 ± 5.24 |
| | TG | 113.3 ± 8.18* | 111.5 ± 9.12** |
| VII–VIII | WT | 126.7 ± 6.23 | 144.5 ± 5.88 |
| | TG | 118.2 ± 9.71* | 125.6 ± 10.01** |
| IX–XII | WT | | 117.4 ± 7.95 |
| | TG | | 105.4 ± 5.40** |

* Values are significantly different ($t$ test, $p < 0.05$).

** Values are significantly different ($t$ test, $p < 0.01$).

[a] Each value represents the mean ± SD of number of round spermatids estimated in at least 40 cross sections.

[b] Each value represents the mean ± SD of number of elongating/elongated spermatids estimated in at least 40 cross sections.

For immunohistochemistry analysis, transgenic males were killed at 16, 28, and 60 (adult) days of age; serial testis sections were immunoprobed with antibodies to HA or with the same HA antibody preabsorbed with its blocking peptide as control. In 16-d-old testis, containing spermatogonia and spermatocytes progressing into the first meiotic phase, no specific immunopositive cells were detected (Figure 6A), whereas in 28-d-old testis round spermatids and elongating spermatids (the ripest type of germ cells present at this stage of the first spermatogenic cycle) were Rap1-HA–immunopositive (Figure 6, B and C). For adult iRap1 testis, differentiating spermatids within the seminiferous epithelium were Rap1-HA immunostained (Figure 6E); into the tubule lumen, where few spermatozoa were visible, Rap1-HA–immunolabeled round spermatids were, however, often detected (Figure 6, E and F). The specificity of the immunostaining was confirmed by the absence of signal in the sections probed with the presaturated antibody (Figure 6D). On the whole, immunohistochemistry has confirmed the testis developmental Rap1-HA immunoblot analysis, and it combined with Table 2 has strengthened the testis morphological analysis; moreover, it has allowed to establish that 1) differentiating haploid germ cells that are prematurely re-

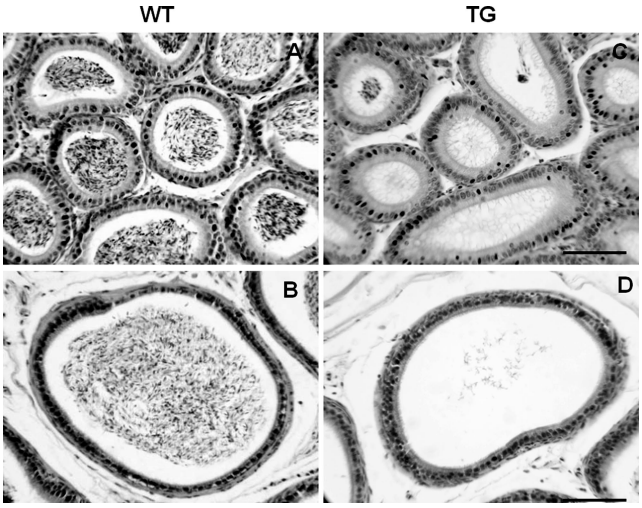


**Figure 5.** Histological comparison between wild-type (WT column) and transgenic (TG column) epididymes. (A and C) Low magnifications providing a general view of sectioned epididymes. (B and D) Higher magnification of a representative cross section from cauda epididimys. Notice the low sperm numbers in the transgenic epididymis. Bar, 65 $\mu$m (A and C) and 19 $\mu$m (B and D).

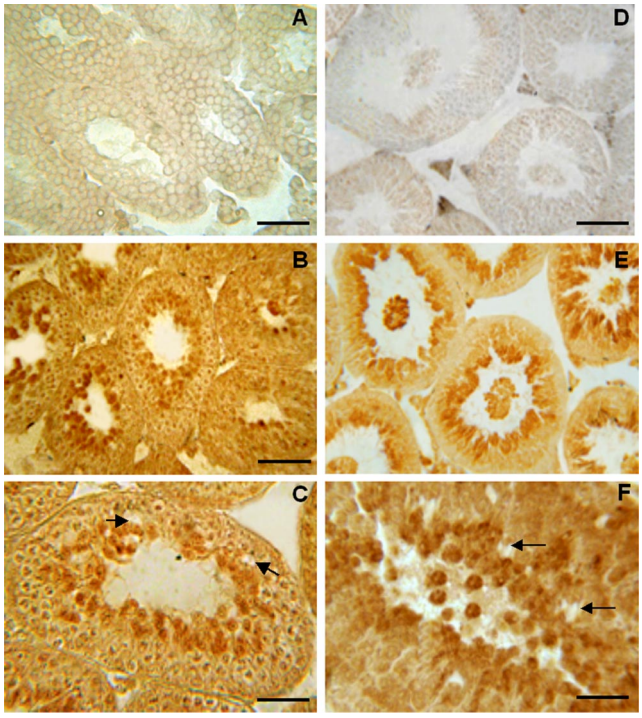


**Figure 6.** Immunocytochemical detection of mutant Rap1-HA. Transgenic testis sections immunostained with HA-antibody. (A) A 16-d-old testis, no HA-immunoreactive cells are detectable. (B and C) A 28-d-old testis. Haploid cells have made their first appearance and are differentiating; these cells are HA-Rap1 immunostained. (D–F) Adult testis. (D) Control section immunostained with presaturated HA antibody. (E and F) Mutant Rap1 is restricted to haploid germ cells, including spermatids immaturely released within the lumen. (C and F) Arrows indicate detachments in cell–cell contacts. Bar, 16 $\mu$m (A), 37 $\mu$m (B), 20 $\mu$m (C), 50 $\mu$m (D and E), and 10 $\mu$m (F).

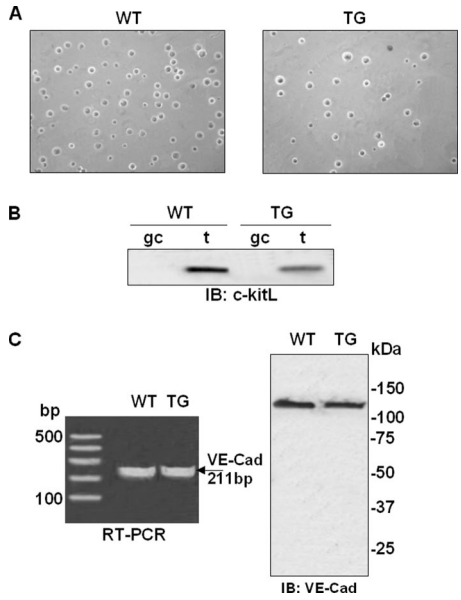


**Figure 7.** VE-cadherin expression in male germ cells. (A) Assessment of purity of germ cell preparations from WT and transgenic (TG) testis by light microscopy under phase contrast. (B) Western immunoblot analysis for the Sertoli cell marker c-kit Ligand; gc, germ cells; t, total testis homogenate. (C) RT-PCR (left) and Western immunoblot (right; 110 $\mu$g/each lane) analysis for VE-cadherin expression in germ cells of wild-type and transgenic mouse.

leased from the epithelium express the mutant protein; and 2) the abnormal retracted spaces observed between spermatids and Sertoli cells occur between HA-immunostained spermatids and the supporting Sertoli cells (Figure 6, C and F, arrows). This scenario, which joins the iRap1 transgenic male mice of all the transgenic lines examined, is consistent with a defect in spermatid–Sertoli cell junction that leads to a release of a fraction of differentiating haploid germ cells.

Indeed, Rap1 has been shown to play a critical role in several aspects of cell adhesion, including VE-cadherin–mediated adherens junctions at the endothelial cell barrier (Bos, 2005). Here, cAMP-Epac-Rap1 signaling works to stabilize adherens junction and to decrease leukocyte migration (Fukuhara *et al*., 2005). So, we have investigated the presence of VE-cadherin in male germ cells.

### *Expression of VE-Cadherin in Male Germ Cells*

ES is a testis-specific type of cell–cell adherens junction; more specifically, the ES found between Sertoli cells at the basal compartment of the seminiferous epithelium is known as the basal ES, whereas that found between Sertoli cells and round, elongating, and elongated spermatids at the adluminal compartment is known as the apical ES (for reviews, see Russell, 1980; Mruk and Cheng, 2004). Albeit the cells that develop, move, and are released are the germ cells, the knowledge in apical ES molecular architecture and regulatory molecules regards essentially the Sertoli cells only (Mruk and Cheng, 2004). Here, we analyzed male germ cells.

First, we assessed the purity of the germ cell preparation used in this study. As shown in Figure 7, germ cell preparations had negligible Sertoli cell contamination as indicated by both light microscopy examination (Figure 7A) and c-kitL immunonegativity (Figure 7B). RNA and proteins extracted from these cell preparations were used for RT-PCR and immunoblotting assays, respectively. As mentioned above,

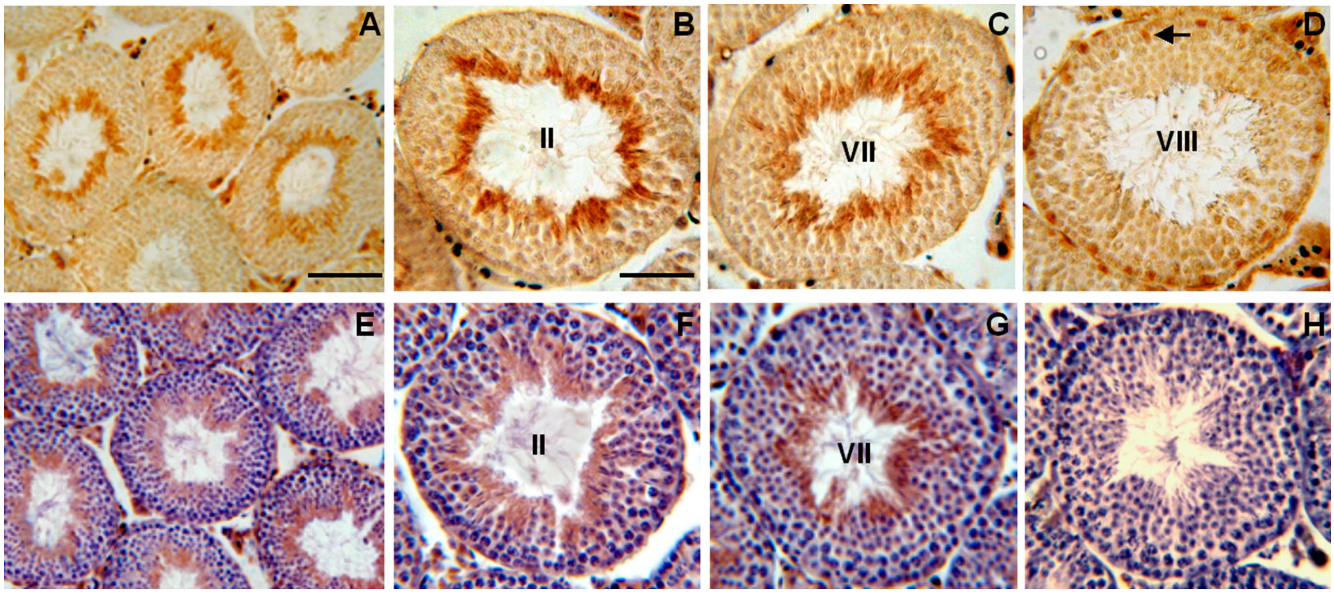


**Figure 8.** Immunocytochemical detection of VE-cadherin in wild-type seminiferous epithelium. (A–G) Representative cross sections of tubules immunostained with the VE-cadherin antibody. (E–G) Sections further counterstained with hematoxylin. (H) Control, treated with preimmune serum and then counterstained with hematoxylin. Numbers inside the tubule lumen indicate the stages of the epithelial cycle. VE-cadherin immunoreactivity is restricted to the haploid population of germ cells; notice the stage specificity of its expression. Arrow in D points to the basal soma of Sertoli cell, that is clearly VE-cadherin positive at stage VIII when spermiation occurs and VE-cadherin is undetectable in germ cells. Bar, 50 $\mu$m (A and E) and 27 $\mu$m (B, C, D, F, G, and H).

among the large group of cell adhesion molecules, we focused our attention on VE-cadherin/mouse cadherin 5, whose expression in seminiferous epithelium so far has not been reported. By using selected primers, VE-cadherin transcript was found in germ cells of both wild-type and transgenic mice (Figure 7C, left); immunoblotting analysis confirmed further the presence of the protein (Figure 7C, right). This is the first experimental evidence that VE-cadherin is expressed by male germ cells.

To expand the biochemical study, immunohistochemistry was used to localize VE-cadherin in adult mouse testis. VE-cadherin was found to localize almost exclusively to the apical compartment of the seminiferous epithelium; it marked round, elongating, and elongated spermatids (Figure 8, A–C), consistent with a localization of the cadherin at the apical ES. Indeed, VE-cadherin expression resulted to be epithelial cycle stage specific. It is high in differentiating spermatids at stage II (Figure 8B) and so remains until the elongated spermatids (step 16) of stage VII (Figure 8C), whereas it is virtually nondetectable at stage VIII (Figure 8D) when spermiation occurs, i.e., when mature spermatids are going to be released or have just been released into the lumen as a consequence of the apical ES disassembly, fundamental to sperm release. At stage VIII, however, the basal soma of Sertoli cells stand out as VE-cadherin–positive foci (Figure 8D, arrow). So, by immunohistochemistry, we showed that not only male germ cells express VE-cadherin but also that this expression keeps pace with the formation and function of apical ESs. This is an important finding, because some controversy still exists as to whether the cadherin/(catenin) complex could represent a functional unit to constitute apical ES in the seminiferous epithelium. Moreover, for example, as determined by immunohistochemistry, the presence of E-cadherin in rat testis is the subject of debate (Lee *et al*., 2003), whereas the localization of N-cadherin between Sertoli cells and spermatids has failed (Andersson *et al*., 1994). In addition, an immunofluorescence study, carried out with a pan-cadherin antibody, has revealed no specific staining for any cadherin molecule detectable at Sertoli cell–germ cell ES during any stage of spermatogenesis (Mulholland *et al*., 2001). We have carried out an immunofluorescence analysis (Figure 9) that has confirmed the immunohistochemistry and provided further interesting details. VE-cadherin immunolabeling within the seminiferous epithelium is confined to the adluminal compartment, at sites coincident with apical ES, and its immunopositivity starts with round spermatids (Figure 9, A and C). The enlargement of Figure 9D allows a better appreciation of the linear and continuous immunolabeling of cell profiles regarding, in particular, round spermatids, whereas in elongating/elongated spermatids that faced to the lumen VE-cadherin seem to localize mainly on the cell junctions of the distal side, where the residual bodies are positioned before their displacement at spermiation, (Figure 9, A–D). Immunofluorescence carried out on isolated germ cells shows that early round spermatids are already positive for VE-cadherin (Figure 9, E–G); late round spermatids (Figure 9, H–K) exhibit a less uniformly diffuse staining, with bright spots concentrated in the head cap.

The immunohistochemical analysis was extended also to the transgenic testis. As shown in Figure 10, the pattern of VE-cadherin expression in the mutant testis is essentially consistent with that of the wild type, being predominantly confined to the apical compartment of the seminiferous epithelium (high at stage II, moderately high at stage VII, and not detectable at stage VIII). Differently from the wild type, however, round and/or elongating spermatids, albeit VE-cadherin immunostained, were found to be dislodging immaturely from the transgenic epithelium and forming, at times, patches of cells that are moving toward the lumen (Figure 10B). In addition, VE-cadherin–positive spermatids were observed within the lumen (Figure 10E).

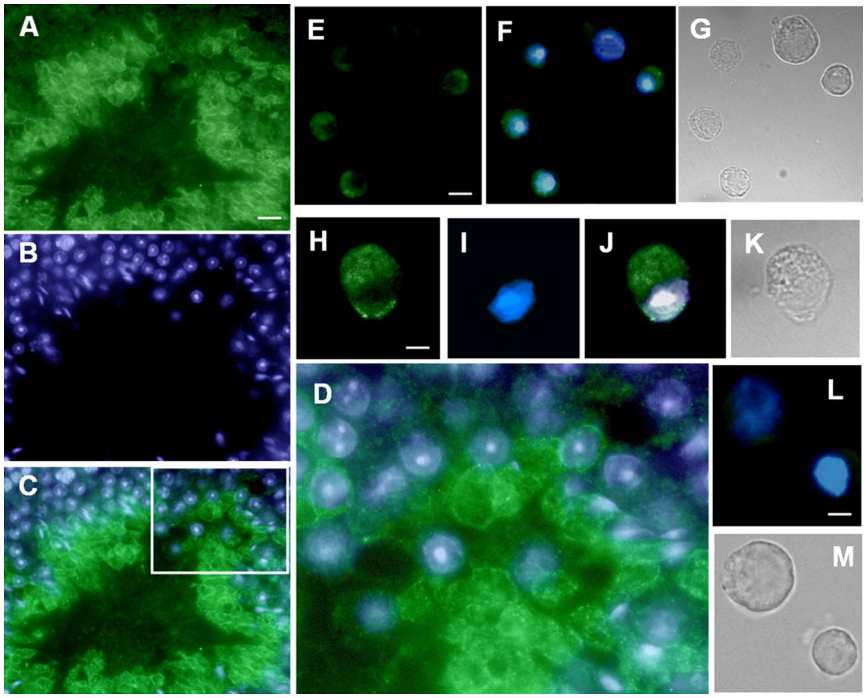


**Figure 9.** Localization of VE-cadherin by immunofluorescence analysis. VE-cadherin (green), DAPI (blue); superimposition of the two fluorochromes (merged images). (A–C) A testis cross section. VE-cadherin (A and C) stains the adluminal compartment where differentiating spermatids are located; the nucleus staining (B and C) allows assessing of differentiation of round-to-elongated spermatids. VE-cadherin signal delineates neatly the cell periphery where there are the regions of contacts between spermatids and Sertoli cells. (D) A 3× magnification of the boxed area in C. (E–M) Spermatogenic cells isolated by enzymatic treatment of testis. (E–G) Round spermatids are VE-cadherin positive, whereas the spermatocyte at the upper of the image is not labeled. (G) Bright field image. (H–K) A late round spermatid that shows a bright VE-cadherin signal, in particular, some spots orderly distributed along the cap head. (K) Bright field. (L–M) Control sample, where L is the merged image, and M is the bright field. Bar, 28 $\mu$m (A–C), 10 $\mu$m (E–G), 4 $\mu$m (H–K), and 6 $\mu$m (L and M).

So, interestingly, in mouse male germ cells VE-cadherin exhibits an expression pattern that is, in part, reminiscent of that of our iRap1. In transgenic testis, both Rap1-HA immunostained and VE-cadherin immunostained undifferentiated spermatids exfoliate into the tubular lumen. Fukuhara *et al*. (2005) reported that the inactivation of Rap1 parallels the inhibition of cell adhesion in vascular endothelial cells. A shift from a strong to a weak state of cell–cell adhesion is known to result in a VE-cadherin solubilization under milder extraction conditions in comparison with those required for VE-cadherin stably associated to the actin cytoskeleton (Lampugnani *et al*., 1997). So, we checked for the solubilization behavior of VE-cadherin in transgenic versus wild-type testes. For this goal, we used transgenic and wild-type testes from 30-d-old mice. At P30, the first round of mouse spermatogenesis has not been accomplished, because the first spermatozoa are not yet released (around P35), but apical ES have been established and are actively engaged in Sertoli–spermatids cell contacts (Russell, 1980; Kluin *et al*., 1982). We set up an experimental procedure that enabled us

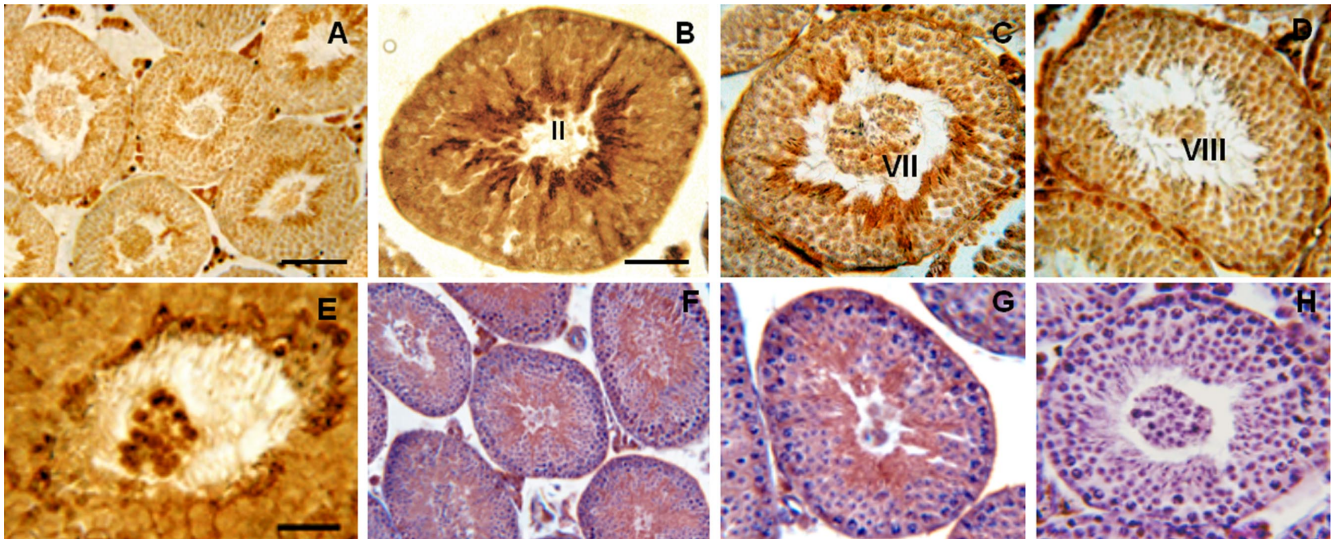


**Figure 10.** Immunocytochemical detection of VE-cadherin in mutant seminiferous epithelium. (A–G) Representative cross sections of tubules immunostained with the VE-cadherin antibody. (F and G) Sections further counterstained with hematoxylin. (H) Control, treated with preimmune serum and then counterstained with hematoxylin. (B–D) For stage-specific immunoreactivity, VE-cadherin exhibits the same pattern as in the wild type. (E) Higher magnification showing exfoliated immature spermatids that are VE-cadherin positive, within the lumen. Bar, 50 $\mu$m (A and F), 16 $\mu$m (B, C, D, G, and H), and 13 $\mu$m (E).

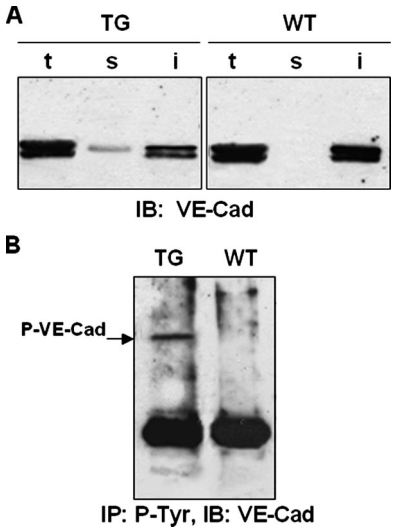


**Figure 11.** Partition of VE-cadherin between soluble and insoluble fractions and its tyrosine phosphorylation in sexually immature testis. (A) Lysates (120 $\mu$g/lane) of TG and WT P30 seminiferous tubules obtained as described in *Materials and Methods* were subjected to SDS-gel electrophoresis and electroblotted to be probed with antibodies to VE-cadherin. t, total homogenate fraction; s, soluble homogenate fraction; and i, detergent homogenate fraction. The soluble homogenate fraction from the transgenic tubules was VE-cadherin positive, whereas in the wild-type VE-cadherin was extracted only under higher detergent conditions. (B) Total homogenate fractions (600 $\mu$g/each) treated with PV (see *Materials and Methods*) from TG and WT P30 seminiferous tubules were immunoprecipitated with anti-phospho-tyrosine antibody, separated by SDS-gel electrophoresis and Western blotted to be probed with antibodies to VE-cadherin. Tyrosine-phosphorylated VE-cadherin (P-VE-cad) was recovered from the TG tubules only. (A and B) Typical results of one of two independent experiments are shown.

to partition VE-cadherin from freshly isolated seminiferous tubules into a soluble and insoluble fraction by a sequential extraction. In Figure 11 A, left, it is shown that although most VE-cadherin was found in the insoluble fraction, a smaller amount was recovered in the soluble fraction from the transgenic seminiferous epithelium, whereas in the wild type (Figure 11A, right), all VE-cadherin was detected in the insoluble fraction. This indicates that in the transgene VE-cadherin association to cytoskeleton elements is weaker. Moreover, tyrosine phosphorylation of VE-cadherin is related to impairment of cell–cell adhesion (Lampugnani *et al.*, 1997; Fukuhara *et al.*, 2006). Tyrosine phosphorylation of VE-cadherin was evaluated in both transgenic and wild-type seminiferous epithelium at P30, i.e., before spermiation. Total protein extracts obtained by inhibiting phospho-tyrosine phosphatases with PV (see *Materials and Methods*) were immunoprecipitated with the anti-phospho-tyrosine antibody; immunoprecipitates were analyzed by SDS gel electrophoresis and Western blotted with the anti-VE-cadherin antibody. As shown in Figure 11B, phospho-tyrosine-containing VE-cadherin was detected only in P30 iRap1 seminiferous epithelium. This suggests a link among expression of interfering Rap1, tyrosine phosphorylation of VE-cadherin, and destabilization of apical ES.

## DISCUSSION

The GTPase Rap1 functions as a critical control element in different cellular processes, including cell adhesion (Reedquist *et al.*, 2000; Knox and Brown, 2002; Enserink *et al.*, 2004; Bos, 2005; Fukuhara *et al.*, 2005; Sakurai *et al.*, 2006), cell differentiation and proliferation (Vossler *et al.*, 1997; Stork and Schmitt, 2002; Kiermayer *et al.*, 2005), and synaptic plasticity (Zhu *et al.*, 2002; Morozov *et al.*, 2003). Such a variety of actions of Rap1 occur via distinct pathways and through factors that are retained to be cell–type-specific (Stork, 2003). Herein, we report the phenotype of the first animal mutant in testis haploid cell Rap1: interfering with Rap1 function leads to reduced fertility consistent with impairment of germ cell–Sertoli cell contacts.

In agreement with our experimental strategy, to interfere, if this was the case, with a spermiogenetic event, the mutant

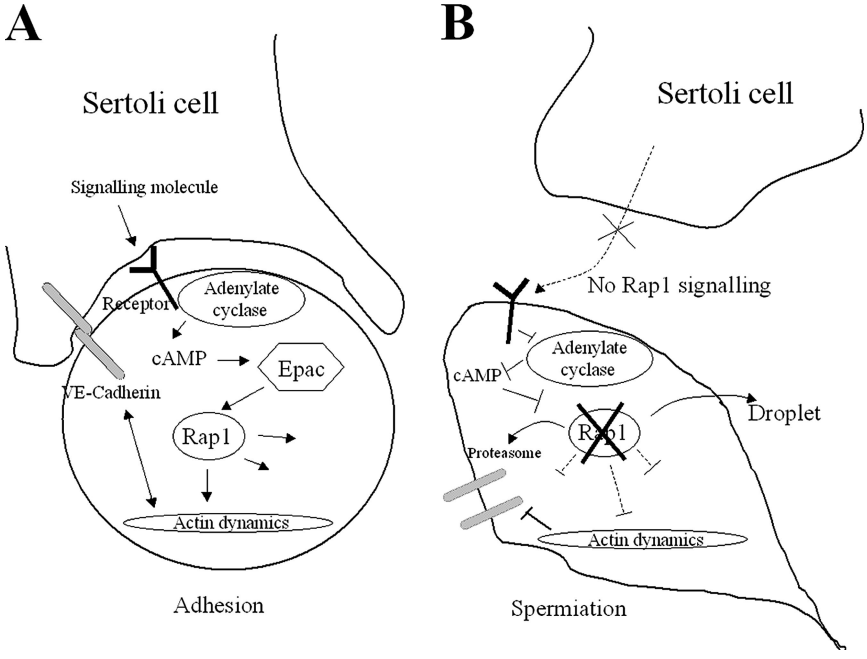


**Figure 12.** Schematic drawing of how Rap1 may regulate spermatid adhesion to the supporting Sertoli cell at the apical ES. (A) A Sertoli cell factor triggers the activation, cAMP/Epac-mediated, of Rap1 in differentiating spermatids. The Rap1-dependent cytoskeletal reorganization promotes and/or enhances VE-cadherin–mediated spermatid–Sertoli cell adhesion. (B) Next to spermiation, Rap1 function is switched off (in terminally differentiated spermatids Rap1 is no more present being eliminated by the way of the cytoplasmic droplet and/or degraded by the proteasome; see Berruti, 2000). Consequently, sperm adhesion at the apical ES is disrupted and spermiation can occur with the release of spermatozoa.

Rap1 protein was effectively expressed only in postmeiotic cells. The iRap1 male mice were severely subfertile, and they showed low counts in epididymal spermatozoa, whereas the transgenic females displayed normal fertility. The fertility parameters reflect the histology of transgenic testes: the lumen of seminiferous tubuli was constantly characterized by an abnormal presence of immaturely released spermatids that, consequently, could not develop to produce mature spermatozoa. In addition and in line with this finding, there were reductions in the expected classes of spermatids within the seminiferous epithelium. Remarkably, immunohistochemistry confirmed that the exfoliated differentiating spermatids express the interfering Rap1 protein.

The histology of the iRap1 transgenic testis is, in part, reminiscent of that described for testosterone-suppressed rat testis (O'Donnell *et al*., 1996), AF-2364–treated rat testis (Wong *et al*., 2005), and conditional null mice depleted in androgen receptor (AR) function from Sertoli cells only (Holdcraft and Braun, 2004). The peculiarity that joins these three animal models is the anomalous detachment of round/elongating spermatids from the seminiferous epithelium combined with spermiation disorders, i.e., the types of defects that characterize our iRap1 mutant. Testicular testosterone is crucial for the differentiation of round to elongated spermatids (McLachlan *et al*., 1994), and it is thought to regulate spermatid–Sertoli cell adhesion (Beardsley and O'Donnell, 2003; Wong *et al*., 2005); its withdrawal, in fact, promotes detachment of round spermatids from rat seminiferous epithelium (O'Donnell *et al*., 1996) and induces spermiation failure (Beardsley and O'Donnell, 2003). In addition, AF-2364, a drug derivative of indazole-3-carbohydrazide, has been extensively used in rats to create an artificial and reversible in vivo model to disrupt Sertoli–germ cell adhesion without affecting hormone serum level (Wong *et al*., 2005). Last, the primary role of Sertoli cell AR function seems to be the regulation of the dynamic of spermatid adhesion to the Sertoli cell (Holdcraft and Braun, 2004). It is, however, yet unknown through which mechanisms and molecular effectors testosterone, AF-2364, and Sertoli–AR work. Notwithstanding the remarkable efforts to dissect molecularly the architecture of testis ES (Mulholland *et al*., 2001; Lee *et al*., 2003; Mruk and Cheng, 2004; Wong *et al*., 2005; Siu *et al*., 2005), the precise mechanism by which the dynamic of this peculiar junction is governed remains largely unexplored.

The transgenic male mice described here express the interfering Rap1[S17N] mutant in haploid germ cells. This dominant-negative mutant has been instrumental in inhibiting endogenous Rap1 in both in vitro (Vossler *et al*., 1997; Schmitt and Stork, 2000) and in vivo (Morozov *et al*., 2003) studies when the GTPase signaling is activated by cAMP. In contrast, Rap1[S17N] mutant has not exhibited potent dominant-negative properties in inhibiting Rap1 when its activation occurs by C3G (van den Berghe *et al*., 1997; Hogan *et al*., 2004). In a recent study devoted to the development of novel potent Rap1 dominant-negative mutants, Dupuy et al. (2005) have confirmed that Rap1[S17N] is able to interfere with the cAMP–Epac-mediated pathway of activation of Rap1, but not with the epidermal growth factor–C3G-mediated pathway. Intriguingly, the cAMP–Epac–Rap1 pathway is known to be the signaling pathway that stabilizes cadherin-mediated cell–cell contacts in the endothelial cell barrier, a well-known organized structure characterized by dynamic adherens junctions (Kooistra *et al*., 2005). Here, in fact, the cAMP–Epac–Rap1 signaling controls cell junction formation when VE-cadherin is involved as the cell adhesion molecule (Kooistra *et al*., 2005). Not only, but the cAMP–Epac–Rap1 pathway has been shown to enhance the VE-cadherin-mediated cell–cell contacts (Fukuhara *et al*., 2005). At the present, there is scanty knowledge about the panel of Rap1-GEFs expressed in male germ cells.

We previously showed that cAMP is able to trigger activation of Rap1 in mouse spermatogenic cells (Berruti, 2003); the search for the presence of the cAMP sensor Epac demonstrated that male germ cells express both Epac isoforms, i.e., Epac1 and Epac2 (Berruti, 2003; Aivatiadou *et al*., 2005). Consequently, a cAMP–Epac–Rap1 signaling could work during spermatogenesis. Because, as remarked above, our iRap1 mutant is restricted to haploid cells, the interference in Rap1 signaling has to affect a spermiogenetic event. The phenotypic and biochemical characterization of the iRap1 male mice has revealed that the spermatid–Sertoli cell adhesion, characterized physiologically by an extensive restructuring, is the affected target. The nature of the junctional adhesion molecule(s) of haploid spermatids involved in ES formation is still elusive, although very recently, significant progresses have been made (Gliki *et al*., 2004; Inagaki *et al*., 2006). We provide here the first evidence that VE-cadherin, a key component of adherens junctions in endothelial cells, is expressed in male germ cells and that, intriguingly, within the seminiferous epithelium, it exhibits a pattern of protein expression strictly related to the timing of apical ES formation and function. Markedly, in the transgenic testis immature spermatids, albeit VE-cadherin positive, exfoliate from the seminiferous epithelium, indicating an impairment in their VE-cadherin–mediated cell adhesion. The biochemical data support this conclusion. First, in P30 transgenic testis, but not in the wild type, VE-cadherin can be partially solubilized under mild extraction conditions; this argues against its strong association to junctional components. Second, in endothelial cells, the loosening of cell–cell contacts is consequence of tyrosine phosphorylation of VE-cadherin (Lampugnani *et al*., 1997; Fukuhara *et al*., 2006); consistently, spermiation, which requires adherens junction disassembling, is known to result in a dramatic increase in phosphotyrosine immunostaining at apical ESs (Chapin *et al*., 2001; Mulholland *et al*., 2001; Siu *et al*., 2003; Zhang *et al*., 2005). Here, we show that, differently from the wild-type littermates, P30 iRap1 seminiferous tubuli contain tyrosine-phosphorylated VE-cadherin.

In conclusion the iRap1 mutant mouse described here could provide an in vivo model to study testis ES dynamic. Figure 12 illustrates a possible role of Rap1 in regulating germ cell–Sertoli cell adhesion. For the first time, a male germ cell protein, specifically the molecular switch Rap1, is shown to play a crucial role in such a vital process. Our findings may have clinical implications for understanding male infertility in humans.

## ACKNOWLEDGMENTS

We thank Johannes Bos (Department of Physiological Chemistry and Center for Biomedical Genetics, University Medical Center Utrecht, The Netherlands) for pMT-2-Rap1S17N-HA plasmid, Toshiaki Noce (Mitsubishi Kagaku Institute of Life Sciences, Minami-Ooya, Machida, Tokyo, Japan) for bPGV-mPI plasmid, and Alfred Wittinghofer (Department of Structural Biology, Max-Plank Institute for Molecular Physiology, Dortmud, Germany) for pCDNA3-Rap1-HA plasmid. We also thank Giorgio Scarì for expert scanning electron microscopy assistance. This work was supported by a COFIN grant and a Fondo Interno per la Ricerca Scientifica 2005 grant (to G.B.).

## REFERENCES

Aivatiadou, E., Brunetti, F., and Berruti, G. (2005). cAMP promotes an Epac2 redistribution where Rap1 is located in differentiating male germ cells. FEBS J. *272 (Supplement 1)*, 326.

Andersson, A. M., Edvardsen, K., and Skakkebaek, N. E. (1994). Expression and localization of N- and E-cadherin in the human testis and epididymis. Int. J. Androl. *17*, 174–180.

Aravindan, G. R., Pineau, C. P., Bardin, C. W., and Cheng, C. Y. (1996). Ability of trypsin in mimicking germ cell factors that affect Sertoli cell secretory function. J. Cell Physiol. *168*, 123–133.

Asha, H., de Ruiter, N. D., Wang, M. G., and Hariharan, I. K. (1999). The Rap1 GTPase functions as a regulator of morphogenesis in vivo. EMBO J. *18*, 605–615.

Beardsley, A., and O'Donnell, L. (2003). Characterization of normal spermiation and spermiation failure induced by hormone suppression in adult rats. Biol. Reprod. *68*, 1299–1307.

Berruti, G. (2000). A novel Rap1/B-Raf/14-3-3 theta protein complex is formed *in vivo* during the morphogenesis differentiation of postmeiotic male germ cells. Exp. Cell Res. *257*, 172–179.

Berruti, G. (2003). cAMP activates Rap1 in differentiating mouse male germ cells: a new signaling pathway mediated by the cAMP-activated exchange factor Epac? Cell Mol. Biol. *49*, 381–388.

Berruti, G., and Martegani, E. (2001). MSJ-1, a mouse testis-specific Dnaj protein, is highly expressed in haploid male germ cells and interacts with the testis-specific heat shock protein Hsp70-2. Biol. Reprod. *65*, 488–495.

Blume-Jensen, P., Jiang, G., Hyman, R., Lee, K. F., O'Gorman, S., and Hunter, T. (2000). Kit/stem cell factor receptor-induced activation of phosphatidylinositol 3′-kinase is essential for male fertility. Nat. Genet. *24*, 157–162.

Bos, J. L. (2005). Linking Rap to cell adhesion. Curr. Opin. Cell Biol. *17*, 123–128.

Chapin, R. E., Wine, R. N., Harris, M. W., Borchers, C. H., and Haseman, J. K. (2001). Structure and control of a cell-cell adhesion complex associated with spermiation in rat seminiferous epithelium. J. Androl. *22*, 1030–1052.

Cooke, H., and Saunders, P. (2002). Mouse models of male infertilità. Nat. Rev. Genet. *3*, 790–801.

De Rooij, D. J., Zwartkruis, F. J., Verheijen, M. H., Cool, R. H., Nijman, S. M., Wittinghofer, A., and Bos., J. L. (1998). Epac is a Rap1 guanine-nucleotide-exchange factor directly activated by cyclic AMP. Nature *396*, 474–477.

Dupuy, A. G., L'Hoste, S., Cherfils, J., Camonis, J., Gaudriault, G., and de Gunzburg, J. (2005). Novel Rap1 dominant-negative mutants interfere selectively with C3G and Epac. Oncogene *24*, 4509–4520.

Enserink, J. M., Price, L. S., Methi, T., Mahic, A., Sonnenberg, A., Bos, J. L., and Tasken, K. (2004). The cAMP-Epac-Rap1 pathway regulates cell spreading and cell adhesion to laminin-5 through the alpha3beta1 integrin but not the alpha5beta4 integrin. J. Biol. Chem. *279*, 44889–44896.

Feig, L. A. (1999). Tools of the trade: use of dominant-inhibitory mutants of Ras-family GTPases. Nat. Cell Biol. *1*, E25–E27.

Fukuhara, S., Sakurai, A., Sano, H., Yamagishi, A., Somekawa, S., Takakura, N., Saito, Y., Kangawa, K., and Mochizuki, N. (2005). Cyclic AMP potentiates vascular endothelial cadherin-mediated cell-cell contact to enhance endothelial barrier function through an Epac-Rap1 signaling pathway. Mol. Cell Biol. *25*, 136–146.

Fukuhara, S., Sakurai, A., Yamagishi, A., Sako, K., and Mochizuki, N. (2006). Vascular endothelial cadherin-mediated cell-cell adhesion regulated by a small GTPase, Rap1. J. Biochem. Mol. Biol. *39*, 132–139.

Giorgini, F., Davies, H. G., and Braun, R. E. (2002). Translational repression by MSY4 inhibits spermatid differentiation in mice. Development *129*, 3669–3679.

Gliki, G., Ebnet, K., Aurrand-Lions, M., Imhof, B. A., and Adams, R. H. (2004). Spermatid differentiation requires the assembly of a cell polarity complex downstream of junctional adhesion molecule-C. Nature *431*, 320–324.

Hogan, C., Serpente, N., Cogram, P., Hosking, C. R., Bialucha, C. U., Feller, S. M., Braga, V. M., Birchmeier, W., and Fujita, Y. (2004). Rap1 regulates the formation of E-cadherin-based cell-cell contacts. Mol. Cell Biol. *24*, 6690–6700.

Holdcraft, R. W., and Braun, R. E. (2004). Androgen receptor function is required in Sertoli cells for the terminal differentiation of haploid spermatids. Development *131*, 459–467.

Ji, M., and Andrisani, O. M. (2005). High-level activation of cyclic AMP signaling attenuates bone morphogenetic protein 2-induced sympathoadrenal lineage development and promotes melanogenesis in neural crest cultures. Mol. Cell Biol. *25*, 5134–5145.

Inagaki, M., Irie, K., Ishizaki, H., Tanaka-Okamoto, M., Miyoshi, J., and Takai, Y. (2006). Role of cell adhesion molecule nectin-3 in spermatid development. Genes Cells *11*, 1125–1132.

Kang-Decker, N., Mantchev, G. T., Juneja, S. C., McNiven, M. A., and van Deursen, J. M. (2001). Lack of acrosome formation in Hrb-deficient mice. Science *294*, 1531–1533.

Kiermayer, S., Biondi, R. M., Imig, J., Plotz, G., Haupenthal, J., Zeuzem, S., and Piiper, A. (2005). Epac activation converts cAMP from a proliferative into a differentiation signal in PC12 cells. Mol. Biol. Cell *16*, 5639–5648.

Kitayama, H., Sugimoto, Y., Matsuzaki, T., Ikawa, Y., and Noda, M. (1989). A ras-related gene with transformation suppressor activity. Cell *56*, 77–84.

Kluin, P. M., Kramer, M. F., and de Rooij, D. G. (1982). Spermatogenesis in the immature mouse proceeds faster than in the adult. Int. J. Androl. *5*, 282–294.

Knox, A. L., and Brown, N. H. (2002). Rap1 GTPase regulation of adherens junction positioning and cell adhesion. Science *295*, 1285–1288.

Kooistra, M. R., Corada, M., Dejana, E., and Bos, J. L. (2005). Epac1 regulates integrity of endothelial cell junctions through VE-cadherin. FEBS *579*, 4966–4972.

Kubota, H., Avarbock, M. R., and Brinster, R. L. (2004). Growth factors essential for self-renewal and expansion of mouse spermatogonial stem cells. Proc. Natl. Acad. Sci. USA *101*, 16489–16494.

Lampugnani, M. G., Corada, M., Andriopoulou, P., Esser, S., Risau, W., and Dejana, E. (1997). Cell confluence regulates tyrosine phosphorylation of adherens junction components in endothelial cells. JCB *110*, 2065–2077.

Lee, N. P., Mruk, D., Lee, W. M., and Cheng, C. Y. (2003). Is the cadherin/catenin complex a functional unit of cell-cell actin-based adherens junctions in the rat testis? Biol. Reprod. *68*, 489–508.

Mashiach, R., Fisch, B., Eltes, F., Tadir, Y., Ovadia, J., and Bartoov, B. (1992). The relationship between sperm ultrastructural features and fertilizing capacity in vitro. Fertil. Steril. *57*, 1052–1057.

McLachlan, R. I., Wreford, N. G., Meachem, S. J., De Kretser, D. M., and Robertson, D. M. (1994). Effects of testosterone on spermatogenic cell populations in the adult rat. Biol. Reprod. *51*, 945–955.

Morozov, A., Muzzio, I. A., Bourtchouladze, R., Van-Strien, N., Lapidus, K., Yin, D. Q., Winder, D. G., Adams, J. P., Sweatt, J. D., and Kandel, E. R. (2003). Rap1 couples cAMP signaling to a distinct pool of p42/44MAPK regulating excitability, synaptic plasticity, learning, and memory. Neuron *39*, 309–325.

Mruk, D. D., and Cheng, C. Y. (2004). Cell-cell interactions at the ectoplasmic specialization in the testis. Trends Endocrinol. Metab. *15*, 439–447.

Mulholland, D. J., Dedhar, S., and Vogl, A. W. (2001). Rat seminiferous epithelium contains a unique junction (Ectoplasmic specialization) with signaling properties both of cell/cell and cell/matrix junctions. Biol. Reprod. *64*, 396–407.

Nagy, A., Gertsenstain, M., Vintersten, K., and Behringer, R. (2003). Manipulating the Mouse Embryo. In: A Laboratory Manual, Cold Spring Harbor, NY: Cold Spring Harbor Laboratory Press.

Nakai, A., Suzuki, M., and Tanabe, M. (2000). Arrest of spermatogenesis in mice expressing an active heat shock transcription factor 1. EMBO J. *19*, 1545–1554.

Oakberg, E. F. (1956). Duration of spermatogenesis in the mouse and timing of stages of the cycle of the seminiferous epithelium. Am. J. Anat. *99*, 507–516.

O'Donnell, L., McLachlan, R. I., Wreford, N. G., de Kretser, D. M., and Robertson, D. M. (1996). Testosterone withdrawal promotes stage-specific detachment of round spermatids from the rat seminiferous epithelium. Biol. Reprod. *55*, 895–901.

Peschon, J., Behringer, R., Brinster, R., and Palmiter, R. (1987). Spermatid-specific expression of protamine 1 in transgenic mice. Proc. Natl. Acad. Sci. USA *84*, 5316–5319.

Reedquist, K. A., Ross, E., Koop, E. A., Wolthuis, R. M., Zwartkruis, F. J., van Kooyk, Y., Salmon, M., Buckley, C. D., and Bos, J. L. (2000). The small GTPase, Rap1, mediates CD31-induced integrin adhesion. J. Cell Biol. *148*, 1151–1158.

Russell, L. D. (1980). Sertoli-germ cell interrelations: a review. Gamete Res. *3*, 179–202.

Sakurai, A., Fukuhara, S., Yamagishi, A., Sako, K., Kamioka, Y., Masuda, M., Nakaoka, Y., and Mochizuki, N. (2006). MAGI-1 is required for Rap1 activation upon cell-cell contact and for enhancement of vascular endothelial cadherin-mediated cell adhesion. Mol. Biol. Cell *17*, 966–976.

Sambrook, J., Fritsch, E. F., and Maniatis, T. (1889). Molecular Cloning: A Laboratory Manual, 2nd ed., Cold Spring Harbor, NY: Cold Spring Harbor Laboratory Press.

Schmitt, J. M., and Stork, P. J. (2000). β2-Adrenergic receptor activates extracellular signal-regulated kinases (ERKs) via the small G protein rap1 and the serine/threonine kinase B-Raf. J. Biol. Chem. *275*, 25342–25350.

Siu, M. K., Mruk, D. D., Lee, W. M., and Cheng, C. Y. (2003). Adhering junction dynamics in the testis are regulated by an interplay of beta 1-integrin and focal adhesion complex-associated proteins. Endocrinology *144*, 2141–2163.

Siu, M. K., Wong, C. H., Lee, N. P., and Cheng, C. Y. (2005). Sertoli-germ cell anchoring junction dynamics in the testis are regulated by an interplay of lipid and protein kinases. J. Biol. Chem. *280*, 25029–25047.

Stork, P. J. (2003). Does Rap1 deserve a bad Rap? Trends Biochem. Sci. *28*, 267–273.

Stork, P. J., and Schmitt, J. M. (2002). Crosstalk between cAMP and MAP kinase signaling in the regulation of cell proliferation. Trends Cell Biol. *12*, 258–266.

van den Berghe, N., Cool, R. H., Horn, G., and Wittinghofer, A. (1997). Biochemical characterization of C3G: an exchange factor that discriminates between Rap1 and Rap2 and is not inhibited by Rap1A(S17N). Oncogene *15*, 845–850.

Vossler, M. R., Yao, H., York, R. D., Pan, M. G., Rim, C. S., and Stork, P. J. (1997). cAMP activates MAP kinase and Elk-1 through a B-Raf- and Rap1-dependent pathway. Cell *89*, 73–82.

Wong, C. H., Xia, W., Lee, N. P., Mruk, D. D., Lee, W. M., and Cheng, C. Y. (2005). Regulation of ectoplasmic specialization dynamics in the seminiferous epithelium by focal adhesion-associated proteins in testosterone-suppressed rat testes. Endocrinology *146*, 1192–1204.

Yamazaki, Y., Fujimoto, H., Ando, H., Ohyama, T., Hirota, Y., and Noce, T. (1998). In vivo gene transfer to mouse spermatogenic cells by deoxyribonucleic acid injection into seminiferous tubules and subsequent electroporation. Biol. Reprod. *59*, 1439–1444.

Zambrowicz, B., Harenda, C., Zimmermann, J., Brinster, R., and Palmiter, R. (1993). Analysis of the mouse protamine 1 promoter in transgenic mice. Proc. Natl. Acad. Sci. USA *90*, 5071–5075.

Zhang, J., Wong, C. H., Xia, W., Mruk, D. D., Lee, N. P., Lee, W. M., and Cheng, C. Y. (2005). Regulation of Sertoli-germ cell adherens junction dynamics via changes in protein-protein interactions of the N-cadherin-beta-catenin protein complex which are possibly mediated by c-Src and myotubularin-related protein *2*, an in vivo study using an androgen suppression model. Endocrinology *146*, 1268–1284.

Zhu, J. J., Qin, Y., Zhao, M., Van Aelst, L., and Malinow, R. (2002). Ras and Rap control AMPA receptor trafficking during synaptic plasticity. Cell *110*, 443–455.

Zwartkruis, F. J., and Bos, J. L. (1999). Ras and Rap *1*, two highly related small GTPases with distinct function. Exp. Cell Res. *253*, 157–165.